

Transition Temperature of Josephson Junction Arrays with Long-Range Interaction

H.R. Shea and M. Tinkham

*Department of Physics and Division of Engineering and Applied Sciences, Harvard University,
Cambridge, MA 02138*

(November 22, 2017)

Abstract

We report measurements of the dependence on magnetic field and array size of the resistive transition of Josephson junction arrays with long-range interaction. Because every wire in these arrays has a large number of nearest-neighbors (9 or 18 in our case), a mean-field theory should provide an excellent description of this system. Our data agree well with this mean-field calculation, which predicts that T_c (the temperature below which the array exhibits macroscopic phase coherence) shows very strong commensurability effects and scales with array size.

74.50.+r

We report an experimental investigation of ordered Josephson junction Arrays with Long-Range Interaction (ALRI), of the sort originally proposed in the disordered limit by Vinokur *et al.*¹ Although such arrays had been fabricated by Sohn *et al.*², the samples used in the present work for the first time have low enough critical currents and hence low enough screening to be in the regime well described by existing theoretical models^{3,4}.

These arrays consist of two perpendicular sets of N parallel superconducting wires, coupled by Josephson junctions at every point of crossing (see Fig. 1). In this geometry, any horizontal (vertical) wire is nearest neighbor to *all* vertical (horizontal) wires, and next-nearest neighbor to *all* other horizontal (vertical) wires. Hence we term the interaction long-range. The number of nearest neighbors in these arrays is equal to the array size N . This is in sharp contrast to standard (short-range interaction) $2D$ arrays where the number of nearest neighbors (typically 4 or 6) is independent of array size.

Arrays with long-range interaction were first proposed as a model for a spin glass for the case where the wires are positionally disordered and a sufficiently strong perpendicular magnetic field is applied¹. More recently, Chandra *et al.*⁴ have shown that even for an *ordered* array, glassy behavior is expected in a very weak field (less than one flux quantum per row). The equivalent of “spins” in these ALRI are the phases of the superconducting wires. Above a transition temperature T_c , the phases of the wires are uncorrelated. However when the array is cooled below T_c , a transition to a macroscopically phase coherent state is predicted to occur.

For an ordered array with long-range interaction in the limit of negligible screening, Sohn *et al.*³ have performed a mean-field analysis and computed the transition temperature $T_c^{MF}(f)$ as a function of the applied field and array size. Because each wire has a large number of nearest-neighbors, a mean-field theory using the phase of each wire as a classical thermodynamic variable should provide a good description of this system. At zero field they find $T_c = NE_J(T = T_c)/2k_B$, where $E_J(T) = \hbar i_c(T)/2e$ and $i_c(T)$ is the (unfluctuated) critical current of a single junction at temperature T . Note the unusual result that T_c should scale with the *size* of the array. To keep T_c of the array well below T_c^{wire} , one requires

$N\hbar i_c^0 \ll 4ek_BT_c^{wire}$, where i_c^0 is $i_c(T=0)$. The computations of Refs. [1], [3], and [4] only hold in the limit of negligible screening, where the array as a whole screens much less than one flux quantum Φ_0 , and in the limit when phase gradients along the wires due to current flow are much less than phase drops at the junctions. The former condition can be written as $N^2L_g i_c^0 \ll \Phi_0$, where L_g is the geometric inductance of a cell in the array. The latter condition can be expressed as $i_c^{junction} \ll i_c^{wire}$. These three inequalities place very strong limits on the magnitude of i_c^0 for given N .

In the experimental work of Sohn and co-workers, $N\hbar i_c^0/4ek_BT_c^{wire} \approx 300$ and $N^2L_g i_c^0/\Phi_0 \approx 10^3$. Hence their samples were not in the regime defined by the above mentioned theories. We present here the first measurements of ALRI with critical currents small enough (of order 5 nA) to be in the limit of extremely weak screening, and to have an array T_c well below the wire critical temperature. Our data show impressive agreement with the mean-field theory, including extremely strong commensurability effects.

The samples consist of 0.25 μm wide Al wires ($T_c^{wire} \approx 1.7$ K) connected by Al-AlO_x-Al junctions, fabricated as follows. A grid-like pattern of lattice constant 2 μm is defined using electron-beam lithography on a PMMA-coated Si wafer. A three-angle shadow evaporation technique is used to deposit both sets of wires sequentially without breaking vacuum, using only the single lithography step. The evaporations are done at 45° to the substrate surface, but at different orientations with respect to the patterned channels. 30 nm of 99.999% pure Al are evaporated in the direction of one set of wires (the “horizontal” set). Al accumulates on the substrate only along those horizontal wires because the PMMA shadows the “vertical” wires. 150 mTorr of O₂ is bled into the chamber, and an oxygen plasma is ignited for 20 minutes to grow an AlO_x barrier. After pumping out the O₂, the sample is rotated so that the second and third evaporations (30 nm of Al each) are done in the direction of the “vertical” wires, going “up” for the second evaporation and “down” for the third, to ensure that the vertical lines are continuous where they “climb” over the horizontal wires. A liftoff completes the process. This shadow evaporation technique yields very high quality underdamped junctions which are a major improvement over those from the previous

fabrication technique.²

The typical single junction resistance is $R_N^{JJ} = 70 \text{ k}\Omega$ which corresponds⁵ to an unfluctuated critical current i_c^0 of 5.6 nA, or $E_J(T = 0)/k_B = 0.13 \text{ K}$. Junction uniformity, measured from single junctions co-fabricated with the arrays, is approximately $\pm 15\%$. The lead configuration is shown in the inset of Fig. 2. Current is injected in the first wire of one set, and extracted from the last wire of that same set. We report data on two arrays: one consisting of 9×9 wires (8×8 cells) and the other of 18×18 wires (17×17 cells).

The arrays are cooled to 315 mK in a ^3He cryostat within a double μ -metal shield which reduces the stray field to less than 50 mG. (A field of 5.2 G corresponds to $f \equiv \Phi_{\text{cell}}/\Phi_0 = 1$ for our $2 \text{ }\mu\text{m}$ spacing). Temperature stability is better than 3 mK below 2 K. A small magnetic field is applied perpendicular to the array using a solenoid surrounding the vacuum can of the cryostat. Screening by the array can be neglected because i_c^0 is so small. Quantitatively, the ratio of the maximum flux screened by the array to the flux quantum is much less than one: $N^2 L_g i_c^0 / \Phi_0 \approx 3 \times 10^{-3} \ll 1$, for $N = 18$ and where $L_g \approx 4 \text{ pH}$ is the geometric inductance of a single cell in the array, modeled as a superconducting square washer.⁶ Considerable care was taken to ensure that the arrays are well shielded from RF and microwave radiation by the use of a shielded room, room-temperature low-pass LC Π -filters, cold resistors, and cold microwave filters.⁷

The current-voltage (I-V) curves for single junctions co-fabricated with the arrays do not show a well-defined critical current at 0.3 K because $E_J < k_B T$, and hence a finite resistance is observed for all bias currents. The arrays on the other hand, consisting of many junctions in parallel, do show, at least at the lowest temperatures, a well-defined critical current and strong hysteresis, as expected from underdamped SIS junctions. Fig. 2 shows an I-V curve for the 17×17 array at $f = 0$. The two jumps in voltage to $2\Delta/e$ and $4\Delta/e$ (where Δ is the superconducting gap) correspond to all the junctions connected to one, then the other, of the current injection wires going normal. The unfluctuated zero-temperature array critical currents $I_c^0 = N i_c^0$ ($\sim 60 \text{ nA}$ for the 9×9 wire array, $\sim 100 \text{ nA}$ for the 18×18 wire array) are so small that the measured I_c will be significantly less than I_c^0 due to thermal fluctuations.

The measured I_c actually corresponds to a jump from a finite-voltage (of order $1\ \mu\text{V}$) phase-diffusion branch⁸ to $2\Delta/e$ at a current value which is affected by damping as well as E_J and T .

We therefore focus instead on the differential resistance $R_d = dV/dI$ (at zero dc bias) as a function of field and temperature since it should be a better measure of the zero-current phase coupling of the array (and hence T_c). R_d is measured using a PAR 124 lock-in amplifier at 15.6 Hz with an excitation current of 0.2 nA (corresponding to $\sim I_c/10$). Fig. 3 shows R_d vs. $f \equiv \Phi_{\text{cell}}/\Phi_0$ plots for several temperatures from 0.3 K to 1.6 K for the 17×17 cell sample. The curves are *not* offset. Because $R_d(f)$ is periodic in f and symmetric around $f = 1/2$, we only plot $R_d(f)$ for f ranging from 0 to $1/2$. $R_d(f)$ displays minima at *all* commensurate fields where $f = p/q$, p and q being integers smaller than N . The $f = 1/17$ and $f = 1/16$ states are not clearly resolved but all other commensurate states are clearly present (such as, for instance, all other multiples of $1/17$, like $2/17$ and $3/17$). *All* the measured positions of the resistance minima are within less than $10^{-4} \times \Phi_0$ from the ideal computed commensurate field values. We observe very similar behavior for the 8×8 cell array, with resistance minima at $f = 1/8, 1/7, \dots$. It is a characteristic feature of ALRI that such strong and detailed structure in the $R_d(f)$ curve is visible. Standard 2D arrays and wire networks do not exhibit such richness of structure because they do not have the long-range order needed to support a stable vortex superlattice with such a large lattice constant (e.g. 17 cells).

The deepest resistance minima occur at the most strongly commensurate states: $f = 0$, $1/2$, $1/3$, $1/4$. The shape of the $R_d(f)$ curve is very similar near all of these states (see Fig. 3). The full widths of the resistance dips (i.e. the field intervals between local maxima on either side of the dips) scale as $1/q$, with $q = 1, 2, 3, \dots$. Near integer f (e.g. $f = 0, 1, 2, \dots$) where $q = 1$, the resistance increases smoothly from $f = n$ until $f = n \pm [1/(N-1)]$, i.e. the first adjacent commensurate state, giving a modulation-free half-width of $1/(N-1)$. Corresponding behavior occurs near other strongly commensurate states.

$R_d(f)$ was measured for 20 temperatures between 0.315 K and 1.8 K, of which 11 are

shown in Fig. 3. As the temperature is increased, $R_d(f)$ increases and the relative amplitudes of the resistance oscillations decrease until at higher temperatures (but with the wires still superconducting) $R_d(f)$ saturates at the normal state resistance of the array $R_N^{array} = 2R_N^{JJ}/18$. In order to extract $T_c(f)$ from the $R_d(f)$ vs. T data, we make use of the finite width of the resistive transition. We *define* the experimental T_c using a resistive criterion; for each field value, R_d is plotted vs. T , and T_c is taken to be the temperature at which R_d interpolates to ϵR_N , and ϵ is a number between 0 and 1. Automating this process produces the top two curves of Fig. 4 of $T_c(f)$ for $\epsilon = 0.5$ (top curve) and $\epsilon = 0.375$ (middle curve). For values of ϵ between approximately 0.4 and 0.8, the inferred T_c scales almost linearly with ϵ .

The bottom curve is the result of a mean-field calculation of $T_c^{MF}(f)$ for a 17×17 cell array. $T_c^{MF}(f)$ is the temperature above which the order parameter $\eta_i \equiv \langle e^{i\phi_i} \rangle$ is equal to 0, where ϕ_i is the phase of the i^{th} wire and the brackets denote a thermal average. There are no free parameters in this calculation, which consists of using an efficient scheme to find the largest eigenvalue of a 17×17 matrix given by Eq. (19) of Ref. [3] for each of one thousand field values shown. The eigenvalue problem is solved assuming a temperature-independent E_J , and T_c^{MF} is finally corrected to account for $E_J(T)$, which varies by $\sim 30\%$ over the temperature range of interest.

The data and mean-field theory curves are in good agreement, both for the 17×17 cell array in Fig. 4, and for the 8×8 cell array (not shown). The maxima in the experimental $T_c(f)$ obviously occur at commensurate fields to the same high accuracy as the minima in the resistive data do, since the critical temperature was extracted from the $R_d(f)$ curves. The mean-field theory also predicts local maxima in T_c^{MF} at all commensurate fields: we find that the positions of the clearly discernible maxima in the experimental $T_c(f)$ and T_c^{MF} agree to better than one part in 10^4 . As can be seen in Fig. 4, the lower resistance criterion gives better quantitative agreement with the mean-field theory T_c^{MF} , which is always below the experimental T_c (and is defined slightly differently). We cannot use a resistive criterion of less than $\epsilon \approx 0.37$ over the whole field range because at low temperatures, for $f \neq 0$,

the array resistance saturates at a non-zero value (up to $\approx 3 \text{ k}\Omega$ for incommensurate f), probably due to macroscopic quantum tunneling of the phases.

In order to compare the experimental T_c 's of the 18×18 wire and 9×9 wire arrays, we must first account for the temperature dependence of E_J in order to obtain T_c^* , the transition temperature one would observe if E_J were constant and the same for both arrays. For $f = 0$ we then obtain $T_{c,18}^*/T_{c,9}^* = 1.9$, using $\epsilon = 0.5$ to determine T_c for both arrays. This is very close to the theoretical value of $18/9 = 2$, indicating that T_c does indeed scale with system size N .

In the absence of screening we can write the following simple expressions for the phases of each wire at $x = ja$ and $y = ka$ at zero applied current:

$$\varphi_k^H = \varphi_0^H + 2\pi f N k$$

$$\varphi_j^V = \varphi_0^V + 2\pi f k j.$$

φ_k^H is the phase of the k^{th} horizontal wire (constant along the wire) and φ_j^V is the phase of the j^{th} vertical wire (depends linearly on the position y along the wire). a is the lattice constant and the vector potential has been chosen as $\mathbf{A} = fx\Phi_0/a^2\hat{\mathbf{y}}$. The only free parameter is $\Delta\varphi_0^{HV} = \varphi_0^H - \varphi_0^V$. The system energy E is

$$E = - \sum_{k,j=0}^{N-1} \cos(\varphi_k^H - \varphi_j^V)$$

The ground state energy is found by minimizing E numerically as a function of $\Delta\varphi_0^{HV}$ for each field. Once $\Delta\varphi_0^{HV}$ is found, all the phase differences are then determined. The local extrema of both $-E_{min}(f)$ and $T_c^{MF}(f)$ occur at exactly the same fields, with very similar relative amplitudes, indicating that the above simple expressions for the phases of the wires do indeed describe the phases very accurately.

It is very difficult to probe the glassiness of this system using transport measurements because the phases unlock as soon as a small transport current is applied. Even though the arrays are biased well below I_c , a finite voltage develops across the system because of phase diffusion. Phase diffusion is unavoidable in the small (i.e. low-capacitance) and weak

junctions required to conform to the model conditions. Since the phases are evolving as $\langle d\varphi/dt \rangle = 2eV_{dc}/\hbar$, they cannot lock. Hence individual metastable states, the presence of which would confirm the presence of a glass, cannot be probed using our transport technique. For instance, we observe the same I_c at every field cool, while trapping into different metastable states should give a range of measured critical currents. Similarly, the T_c we measure reflects an average over many configurations and thus reveals very little about the glassiness of the array.

In conclusion, we have fabricated Josephson junction arrays with long-range interaction and extremely weak critical currents. A mean-field theory provides an excellent description of this system because every wire has a large number of nearest-neighbors (9 or 18 for the arrays presented here). Our data for $T_c(f, N)$ are in very good agreement with the mean-field calculation: we find that $T_c(f = 0)$ scales with system size and observe very strong commensurability effects. The array differential resistance at zero dc bias exhibits minima at *all* commensurate fields, displaying far more complex, but well understood, structure than standard 2D arrays or wire networks.

We wish to thank R.J. Fitzgerald and M.A. Itzler for their extensive assistance with the measurements and analysis, and J.M. Hergenrother, D. Davidovic, and M.S. Rzchowski for their insightful comments. H.R.S. acknowledges support of NSERC of Canada and FCAR du Québec fellowships. This work was supported in part by ONR Grant No. N00014-96-1-0108, JSEP Grant No. N00014-89-J-1023, and NSF Grant No. DMR-92-07956.

REFERENCES

- ¹ V. M. Vinokur, L. B. Ioffe, A. I. Larkin, and M. V. Feigel'man, Zh. Eksp. Teor. Fiz. **93**, 343 (1987) [Sov. Phys. JETP **66**, 198 (1987)]
- ² L. L. Sohn, M. T. Tuominen, M. S. Rzchowski, J. U. Free, and M. Tinkham, Phys. Rev. B **47**, 975 (1993)
- ³ L. L. Sohn, M. S. Rzchowski, J. U. Free, and M. Tinkham, Phys. Rev. B **47**, 967 (1993)
- ⁴ P. Chandra, L. B. Ioffe, and D. Sherrington, Phys. Rev. Lett. **75**, 713 (1995); P. Chandra, M. V. Feigelman, and L. B. Ioffe, Phys. Rev. Lett. **76**, 4805 (1996)
- ⁵ V. Ambegaokar and A. Baratoff, Phys. Rev. Lett. **10**, 486 (1963); erratum, **11**, 1044 (1963)
- ⁶ J. M. Jaycox and M. B. Ketchen, IEEE Trans. Magn. **MAG-17**, 400 (1981)
- ⁷ J. M. Martinis, M. H. Devoret, and J. Clarke, Phys. Rev. B **35**, 4682 (1987)
- ⁸ J. M. Martinis and R. L. Kautz, Phys. Rev. Lett. **63**, 1507 (1989); R. L. Kautz and J. M. Martinis, Phys. Rev. B **42**, 9903 (1990)

FIGURES

FIG. 1. Schematic drawing of a 2 wire by 3 wire array with long-range interaction. There are Josephson junctions at every crossing point of the superconducting wires.

FIG. 2. Voltage-Current plot at 0.315 K in zero field of the 17×17 cell array. The dashed line corresponds to sweeping current up, the solid line to sweeping current down. There is a finite slope at zero bias, too small to be seen on the graph. The inset is a schematic diagram of the lead configuration used for current injection and voltage measurement.

FIG. 3. Plot of zero-bias differential resistance of the 17×17 cell array vs. normalized flux f , measured with a 0.2 nA ac excitation, for selected temperatures. The curves are *not* offset. From the lowest to the highest curve, the temperatures are: 0.417 K, 0.702 K, 0.797 K, 0.959 K, 1.047 K, 1.13 K, 1.212 K, 1.288 K, 1.39 K, 1.51 K, and 1.69 K. The local minima in resistance occur within $10^{-4} \times \Phi_0$ of all the commensurate flux values, i.e. at *all* $f = p/q$ where p and q are integers between 1 and 17.

FIG. 4. Plot of the temperature T_c corresponding to the onset of macroscopic phase coherence vs. normalized flux f for the 17×17 cell array. The top two curves (data) are computed from the differential resistance vs. field data by using a resistive transition criterion for T_c of $0.5R_N^{array}$ (top curve) and $0.375R_N^{array}$ (middle curve). The lower curve is the result of a mean-field calculation of $T_c^{MF}(f)$.

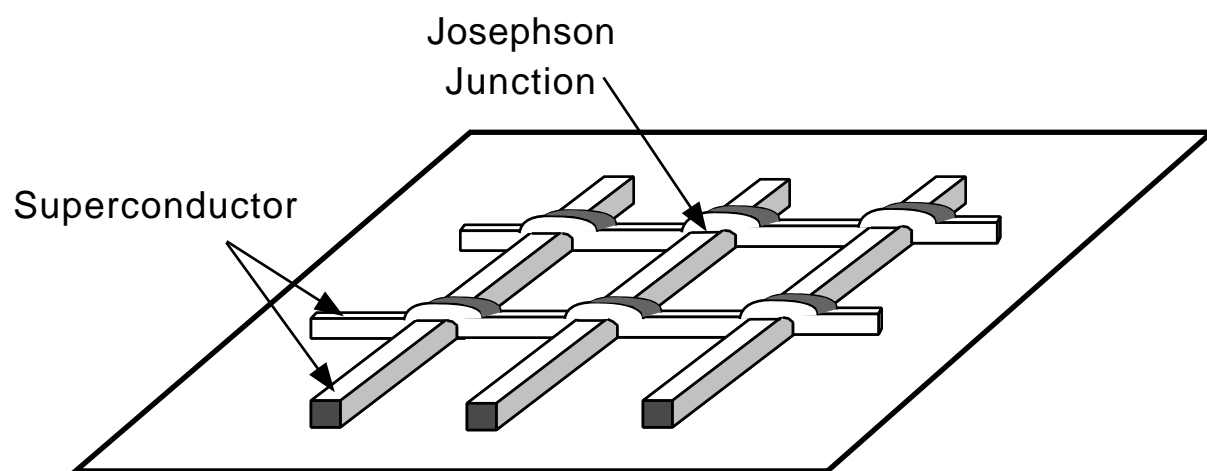


FIGURE 1

H.R. Shea and M. Tinkham
"Transition Temperature of Josephson Junction
Arrays with Long-Range Interaction"

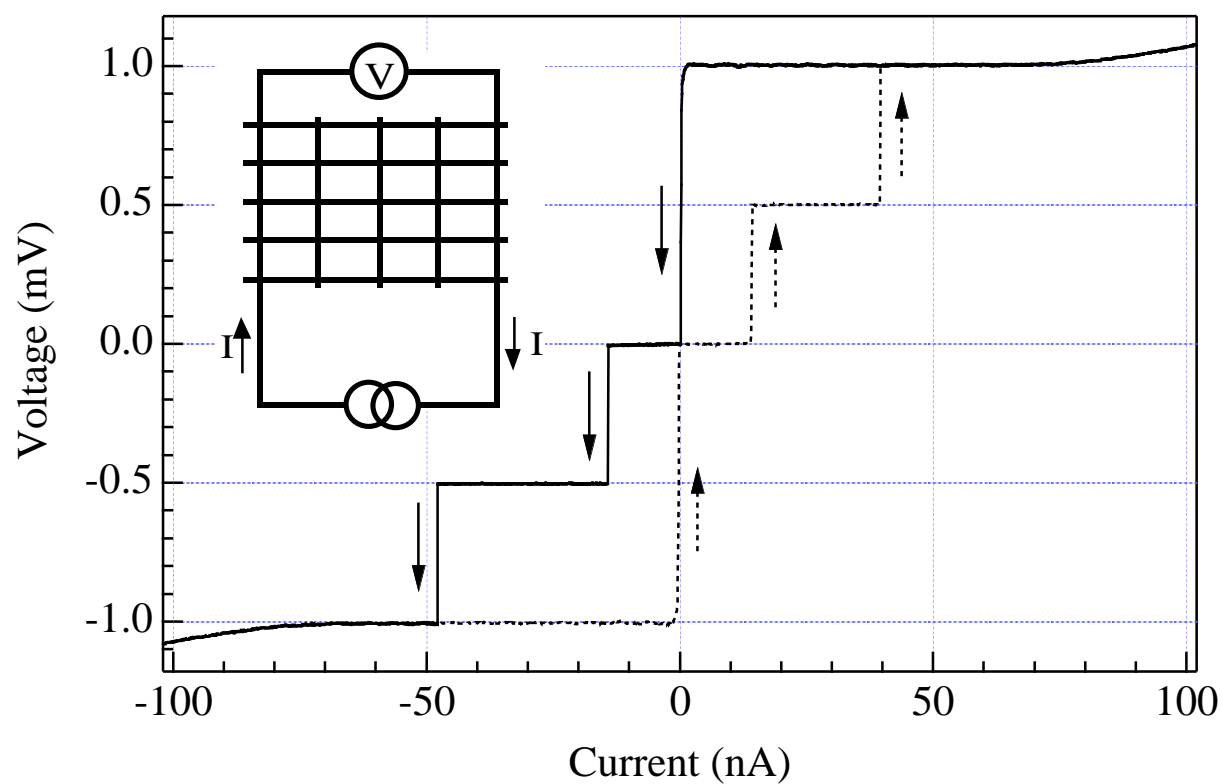


Figure 2

H.R. Shea and M. Tinkham
 "Transition Temperature of Josephson Junction Arrays
 with Long-Range Interaction"

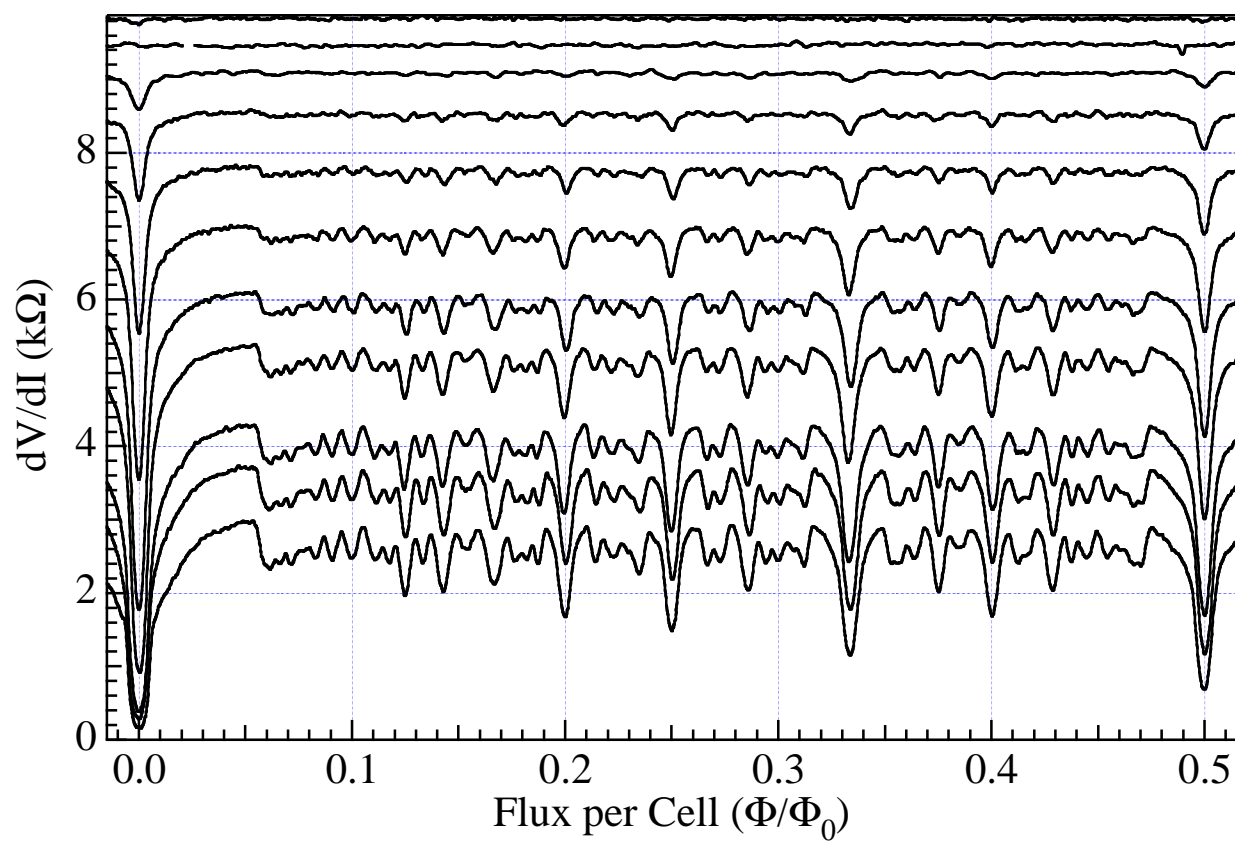


Figure 3

H.R. Shea and M. Tinkham
 "Transition Temperature of Josephson Junction Arrays with Long-Range Interaction"

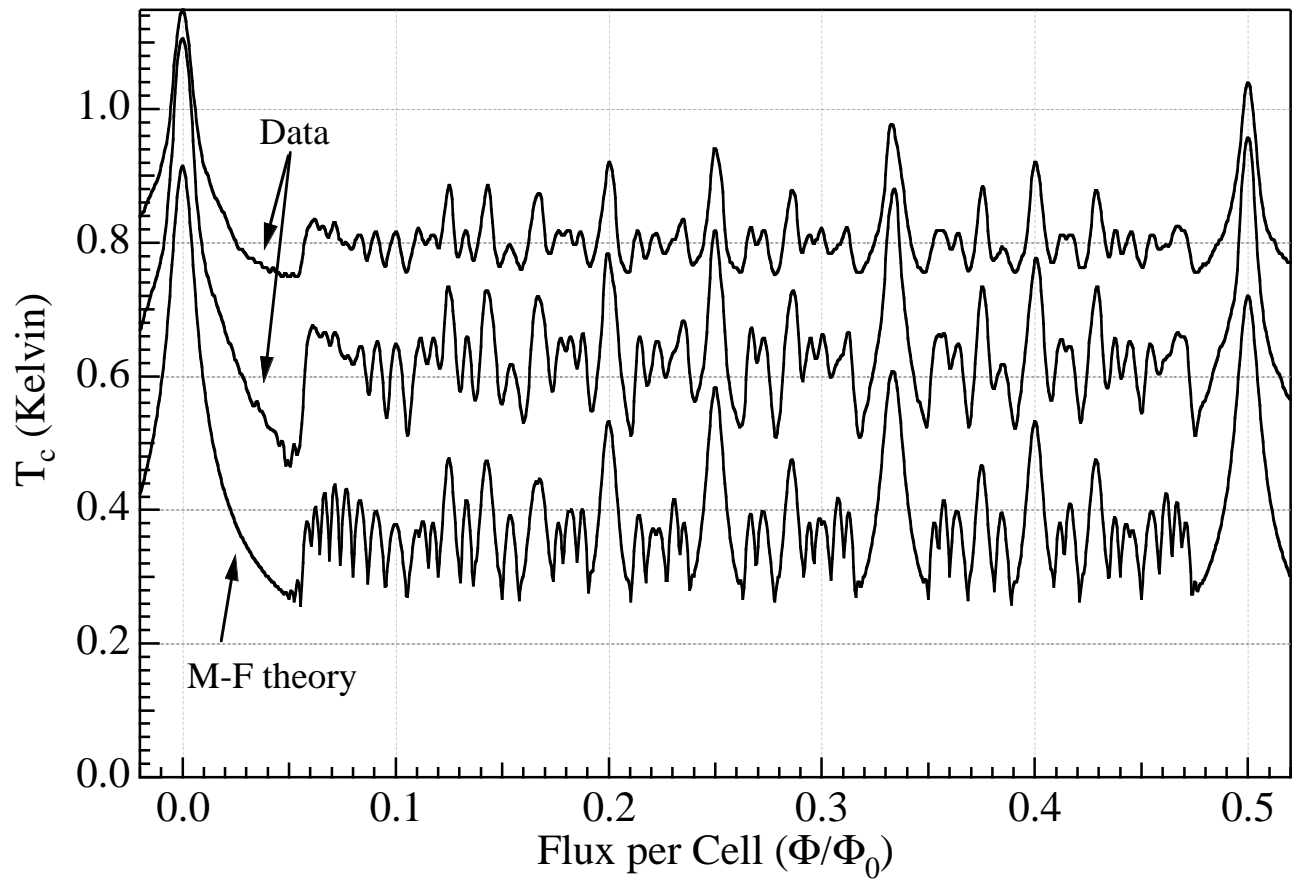


Figure 4

H.R. Shea and M. Tinkham
 "Transition Temperature of Josephson Junction Arrays with Long-Range
 Interaction"